

## **Novel exsolution method for processing composite cathodes for proton conducting ceramic fuel cells**

*Laura Rioja-Monllor<sup>a,†</sup>, Carlos Bernuy-Lopez<sup>a,†</sup>, Marie-Laure Fontaine<sup>b</sup>, Tor Grande<sup>a</sup> and Mari-Ann Einarsrud<sup>a</sup>*

<sup>a</sup> Department of Materials Science and Engineering, NTNU Norwegian University of Science and Technology, 7491 Trondheim, Norway. tor.grande@ntnu.no (T.G.); mari-ann.einarsrud@ntnu.no (M.A.E.)

<sup>b</sup> SINTEF Industri, 0314 Oslo, Norway. Marie-Laure.fontaine@sintef.no

<sup>†</sup>Current address: AB Sandvik Materials and Technology, R&D, 81181 Sandviken, Sweden. laura.rioja-monllor@sandvik.com (L.R.M.); carlos.bernuy-lopez@sandvik.com (C.B.L.)

The measurement of the average grain size of the LB and BZ phases were done as follows. The  $d_{hkl}$  distances were extracted from the HRTEM images by measuring an area of interest from the images with fast Fourier transform analysis, and calculating the average distance over more than ten consecutive  $hkl$  planes. The identification of the composite phases was done by direct comparison of the  $d_{hkl}$  distances with the  $d_{hkl}$  distances calculated from XRD.

The grain size analysis included the grains where the grain boundaries were clearly defined counting; 52 grains for Cexs and 119 grains for Cdir. Examples of TEM images are presented in the images in Figure S1. The red and blue eye-guiding lines represent the microstructural conformation of the particles.

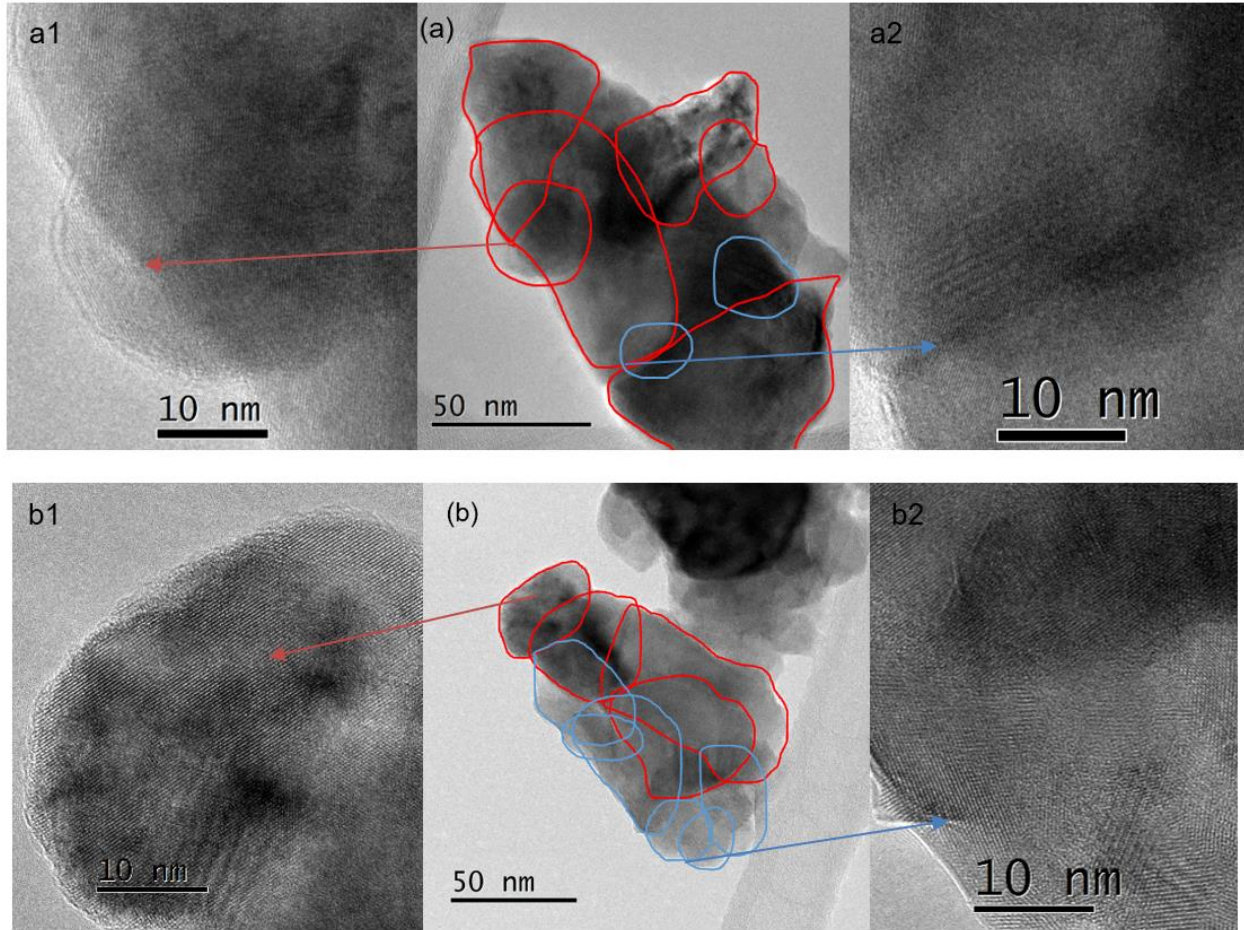
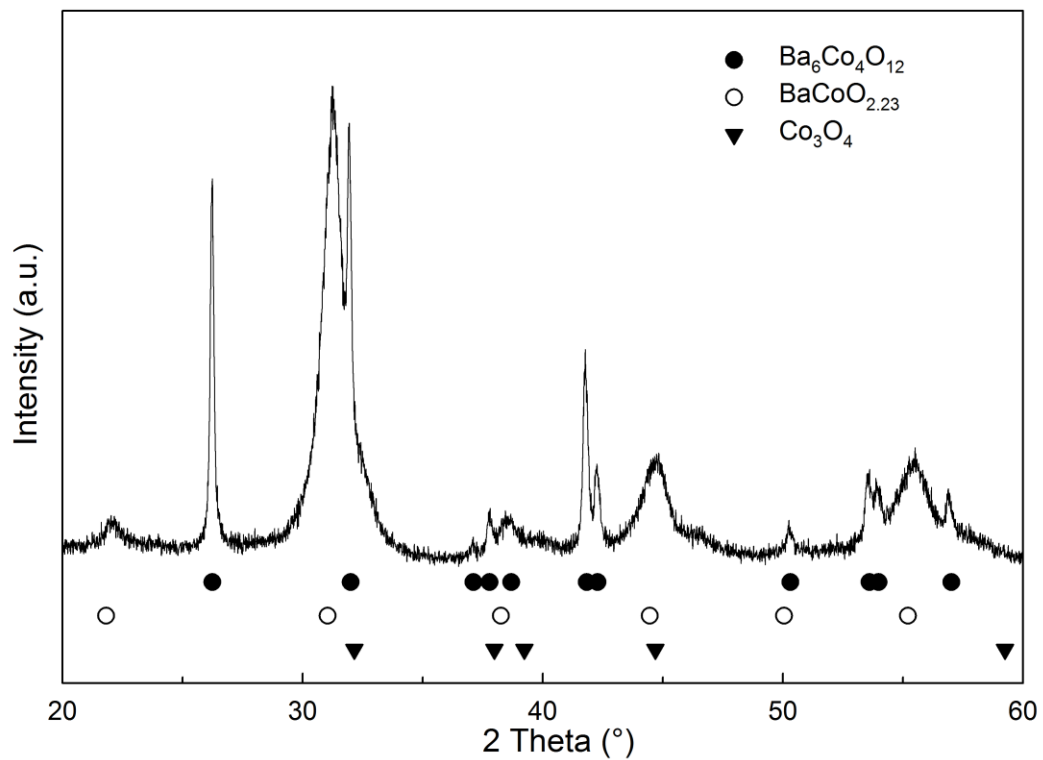


Figure S1. TEM micrographs of the composite by exsolution (a) and the direct composite (b). Agglomerates of BZ- and LB-based phases are shown. The approximate circumference of the grains of BZ-based phase (red) and LB-based phase (blue) are marked as guide for the eye. HRTEM images of selected grains or grain boundaries are included in the a1, a2, b1 and b2 figures.

Figure S2 demonstrates that the transient phase formed at 750 °C is not stable phase when cooled to room temperature. The main phase observed is the perovskite structure transient phase with broad diffraction lines. In addition, the decomposition products La and Zr doped cubic  $\text{BaCoO}_{2.23}$ , polymorphs of hexagonal  $\text{BaCoO}_x$ , and cobalt oxide were identified. The mismatch of the ionic radii of the cobalt  $\text{Co}^{3+}/\text{Co}^{4+}$  at the B-site, ( $\text{Co}^{3+}$ : 0.61 Å and  $\text{Co}^{4+}$ : 0.53 Å) compared to Zr (0.72 Å) in oxidizing conditions results in the formation of secondary phases where cobalt is expelled out of the main cubic perovskite structure.



**Figure S2.** XRD pattern of the transient phase after cooling from 750 °C to room temperature in synthetic air. The positions of the main diffraction lines of the identified phases are given.

Figure S3 shows the electrical conductivity corrected for the porosity of both Cexs and Cdir composites. The electrical conductivity was corrected by using Bruggeman model. The conductivity of the fully dense samples is given by  $\sigma = \sigma_m \cdot (1-x)^{-3/2}$ , where  $\sigma_m$  is the measured conductivity and  $x$  is the volume fraction of pores.

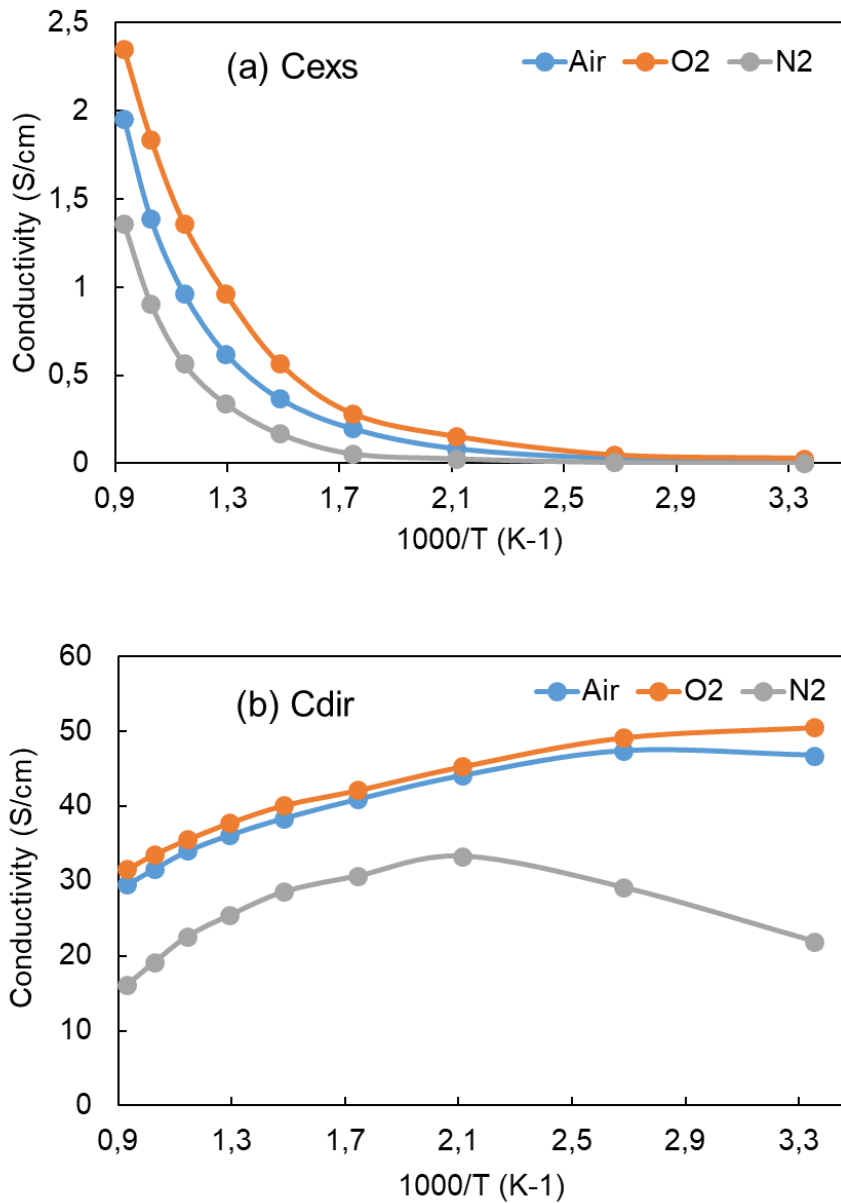


Figure S3. DC conductivity as a function of temperature of (a) Cexs and (b) Cdir composites corrected for the porosity measured by 4-probe method. The electrical conductivity was measured in dry gases. Lines are guides for the eye.